전력전자학술대회 논문집 2000. 7.19-22

Power Factor Correction of Three Phase Voltage Source PWM Converter for Inverter Arc Welding Machine

Hae-Ryong Choi, Hong-Sung Kim, Seong-Yo Lee Hyung-Soo Mok, Gyu-Ha Choe,
Department of Electrical Engineering, Konkuk University

ABSTRACT

Diode rectifier has been widely used as the preregulator of inverter arc welding machine(IAW). As it is linked to power utility, a disorder of other instruments can be burst out. The adoption of voltage source PWM converters can be considered, and which must catch the compromise of between performance and cost. So, in this paper voltage source PWM converters which have single(i.e. SMR) and six(i.e. PWM converter) control switch respectively, are analyzed and evaluated through digital simulation and experiment. In addition the improved input characteristics of IAW are shown and compared to those of conventional one.

1. Introduction

An IAW consists of preregulator part, inverter part , transformer and postregulator. Because conventional Inverter welding machine uses diode rectifier as preregulator and then load varies remarkably, it results in low power factor and unstale inverter operation. Among many problems, low-order harmonics and output voltage ripple must be considered deliberately because these problems deteriorate utility quality and total system performance. As countermeasure, the control techniques optimizing utility condition and improving dynamic response can be considered[1-6]. So, it is proper to apply a voltage fed PWM converter with single and six control switch respectively. A tradeoff is established between cost and performance. In this paper IAW adopting single or six switch PWM converter is reviewed in terms of power factor. Additionally the comparison of two kinds of IAW have been reported for size, weight and cost.

2. Load Characteristics

The drooping characteristic is dominant over the arc-load. The optimal relation of arc voltage and arc current is obtained from Eq. (1). The effect according to welding conditions is depicted in Fig.(2). Though the variations of arc condition, the slope of arc-power is constant approximately.

$$V = V_0 + mI \quad \Rightarrow \quad \frac{dI}{dV} = \frac{1}{m} \tag{1}$$

where

V : arc voltage I: arc current

V_0 : initial value of arc voltage

m : optimal slope

The arc power versus arc voltage is given by following:

$$\frac{d}{dV}(VI) = I + V\frac{dI}{dV} = I + \frac{1}{m}V \tag{2}$$

As the perturbation of arc length has no relation with welding heat, the line with drooping characteristics is expressed as Eq. (3). When we set a welding condition (I_1, V_1), the optimal slope(m) is $-\frac{V_1}{I_1}$.

$$V = V_0 - \frac{V_1}{I_1}I \tag{3}$$

As a result, the operating point that meets the arc characteristics and the welding source has constant slope as welding power increases. In welding process, arc-regeneration is repeated

with 20[Hz](200A). To supply dc-power safely, a 50% rated power must be considered as the load variation.(Fig.3)

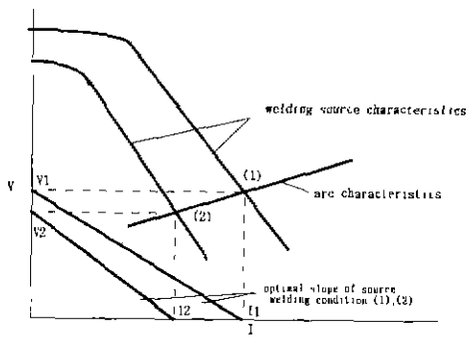

Fig. 2 Effect according to welding conditions

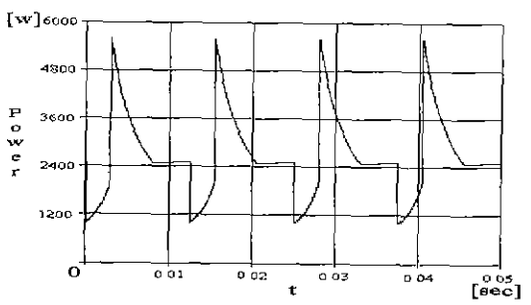

Fig. 3 Instantaneous power variation of IAW.

3. Voltage Source PWM Converter

3.1 three phase SMR

3.1.1 operation

Like in Fig.4, a SMR constitutes input filter(Lf - Cf), boost reactor, switch(Sb) and blocking diode(Db). Based upon the theory of DC-DC boost converer, the SMR can obtain excellant filtering performance with less reactive component by harmonic conversion from low order to high order.

The operation is divided by On-Time state and Off-Time state. State equations on On-Time state are given by

$$V_{PO}=-L\frac{di_a}{dt}+V_a=-L\frac{di_b}{dt}+V_b=-L\frac{di_c}{dt}+V_c \quad (4)$$

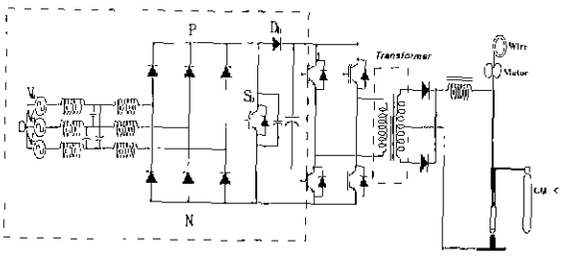

(a) configuration

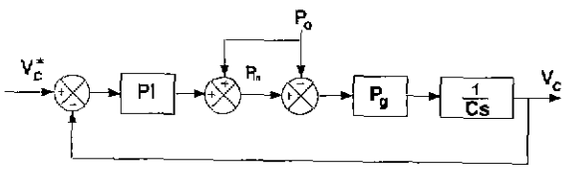

(b) control block diagram

Fig. 4 Proposed IAW(I).

Also, during Switch Off-Time, state equations are expressed as Eq.(5) respectively.

$$\begin{aligned} V_{PO}-V_a&=-L\frac{di_a}{dt}\\ V_{PO}-V_b-V_o&=-L\frac{di_b}{dt}\\ V_{PO}-V_c&=-L\frac{di_c}{dt}\end{aligned} \quad (5)$$

Reflecting on Eq. (3)(4)(5), the variables affecting power factor are boost inductor and voltage gain(M) under constant frequency and load. Eq. (6), and Fig.5 shows the boundary of duty dependent on selected voltage gain(M).

$[0\le\omega t<\frac{\pi}{6}]$

$$I_A=\frac{\sin(\omega t)}{\sqrt{3}M-3\sin(\omega t)}\frac{V_oT_{ON}^2}{2LT_{SW}} \quad (6)$$

$[\frac{\pi}{6}\le\omega t<\frac{\pi}{3}]$

$$I_A=\frac{M\sin(\omega t)+\frac{1}{2}\sin(2\omega t-\frac{2\pi}{3})}{[\sqrt{3}M-3\sin(\omega t+\frac{2\pi}{3})][M-\sin(\omega t+\frac{\pi}{6})]}\frac{V_oT_{ON}^2}{2LT_{SW}} \quad (7)$$

$[\frac{\pi}{3}\le\omega t<\frac{\pi}{2}]$

$$I_A=\frac{M\sin(\omega t)+\sin(2\omega t+\frac{2\pi}{3})}{[\sqrt{3}M+3\sin(\omega t+\frac{2\pi}{3})][M-\sin(\omega t+\frac{\pi}{6})]}\frac{V_oT_{ON}^2}{2LT_{SW}} \quad (8)$$

where $M=\frac{V_o\ (dc\ link\ voltage)}{\sqrt{3}V_{LN}\ (peak\ value\ of\ L-L\ voltage)}$ (9)

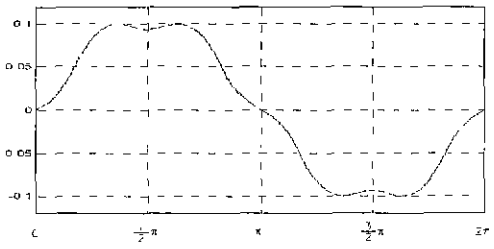

Fig. 5 Input current of 3-phase SMR

It is clear from Fig.5 that high value of M yields Continuous Conduction Mode(CCM). On the contrary low value of M yields Discontinuous Conduction Mode (DCM). Through input current analysized by numerical method, one knows that higher value of M causes the more sinusoidal waveform in Fig.6.

$$d_b = 1 - \frac{1}{M} \tag{10}$$

where d_b : boundary duty of CCM and DCM

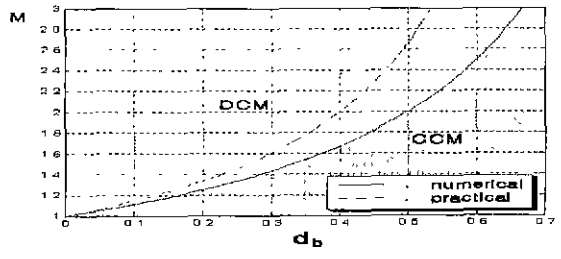

Fig. 6 Boundary condition of 3-phase SMR

3.1.2 voltage controller

State equation considering dc link input-output power is as follows.

$$C\frac{dV_c}{dt} = i_i - i_o = \frac{P_{in}}{V_c} - \frac{P_o}{V_c} \tag{11}$$

where

P_{in}: dc link input power, P_o: dc link output power

Also, the linealized model of dc output port is as follow.

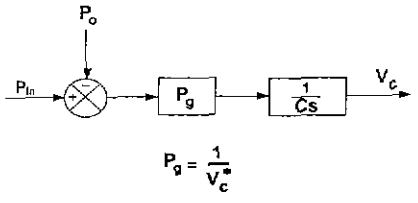

Fig. 7 Linearized dc side model

Because there is not a current controller in SMR, just a voltage controller is designed with PI controller.

$$P_{in}^* = (k_{pv} + \frac{k_{iv}}{s})(V_c^* - V_c) + V_c i_o \tag{12}$$

The transfer function of voltage controller is as follows.

$$\frac{V_c}{V_c^*} = \frac{\frac{P_g k_{pv}}{C} s + \frac{P_g k_{iv}}{C}}{s^2 + \frac{P_g k_{pv}}{C} s + \frac{P_g k_{iv}}{C}} \tag{13}$$

where k_{pv}: propotional gain, k_{iv} : integral gain

3.2 three phase PWM converter

3.2.1 operation

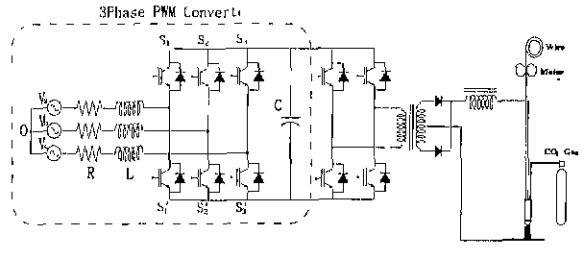

(a) configuration

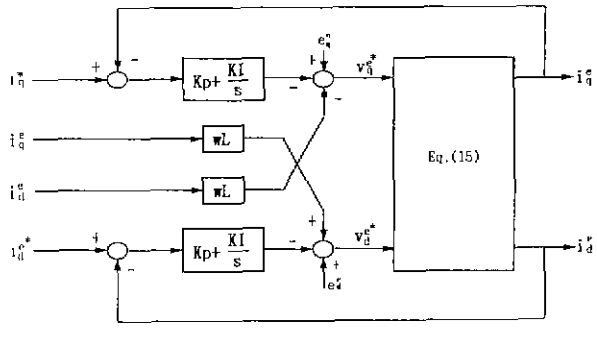

(b) cotrol block diagram

Fig. 8 Proposed IAW.(II)

A PWM converter has a function of bi-directional power flow. To balance power supply, a voltage controller using PI or IP controller produces current reference signal voltage. Input power supplied from source can be represented as the sum of load and system loss.

Table 3. Comparisons of volume, weights and costs of IAWs.

	inductor [cm^3]	capacitor [cm^3]	controller [cm^3]	power [cm^3]	total volume [cm^3]	total weight [kg]	cost
conventinal IAW	3067	196.34	500	7406	70000	50	low
IAW with SMR	5067	392.68	628	8410	75000	58	medium
IAW with PWM	5587	96.34	920	8810	77500	60	high

$$P_{in} = P_L + P_{Loss} \tag{14}$$

where P_{in} : input power
P_L : load
P_{Loss} : system loss

$$\begin{bmatrix} Pi_q^e \\ Pi_d^e \end{bmatrix} = \begin{bmatrix} -\frac{R}{L} & \omega \\ -\omega & -\frac{R}{L} \end{bmatrix} \begin{bmatrix} i_q^e \\ i_d^e \end{bmatrix} + \begin{bmatrix} -\frac{1}{L} & 0 \\ 0 & -\frac{1}{L} \end{bmatrix} \begin{bmatrix} v_q^e - e_q^e \\ v_d^e \end{bmatrix} \tag{15}$$

where P: differential operator

A input reference current given by the relation of complex power can be expressed as

$$\begin{bmatrix} i_q^e \\ i_d^e \end{bmatrix} = \frac{2}{3(V_q^{e^2} + V_d^{e^2})} \begin{bmatrix} V_q^e & -V_d^{e^2} \\ V_d^{e^2} & V_q^e \end{bmatrix} \begin{bmatrix} P_{in} \\ Q \end{bmatrix} \tag{16}$$

$$\begin{bmatrix} i_q^e \\ i_d^e \end{bmatrix} = \begin{bmatrix} \frac{2P_{in}}{3V_q^e} \\ 0 \end{bmatrix} \tag{17}$$

If Q is set zero, q-axis current required from source is obtained. This result shows the control of q-axis current leads to dc-link voltage.

3.2.2 PI controller in rotating cordinate

A PI controller in rotating cordinate can be designed as follows.

$$V_q^{e^*} = -\left(K_{ap} + \frac{K_{qi}}{s}\right)(i_q^{e^*} - i_q^e) - \omega \hat{L} i_d^e + V_q^e \tag{18}$$

$$V_d^{e^*} = -\left(K_{ap} + \frac{K_{qi}}{s}\right)(i_d^{e^*} - i_d^e) + \omega \hat{L} i_q^e + V_d^e \tag{19}$$

Assuming source voltages are balanced, input variables can be translated into dc values.

4. Simulation & Experiment

4.1 simulation

Table 1. Constants selection for SMR.

source(rms)	220[V]
boost inductor & resistor	0.1[mH] , 0.1[Ω]
dc capacitor	3300[μF]
reference dc voltage	400[V]
voltage controller constant (ζ_v , ω_v)	0.707 , 30

Table 2. Constants selection for PWM converter.

input voltage(rms)	220[V]
input inductance & resistance	3.1[mH] , 0.2[Ω]
sampling time	8[kHz]
FFT data sample number	2048
dc capacitpor	3300[μF]
dc voltage	400[V]
current controller constants (ζ_i , ω_i)	0.707 , 600
voltage controlcer constants (ζ_v , ω_v)	0.707 , 30

A simulation is accomplished by PSIM(Power Simulation) and ACSL(Advanced Continuous Simulation Language) which have rapid calculation speed using ideal and simplified model, and that verify theoretical approach. Maximum power and load characteristics of inverter arc welding machine are approximated as Fig 3. Input/Output waveforms and harmonics spectrums by simulation are represented to well fit with theoretical expression. The constants used at simulation are like Table 1 and 2.

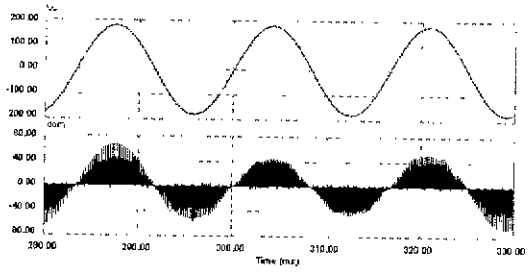

(a) input waveform operating in DCM

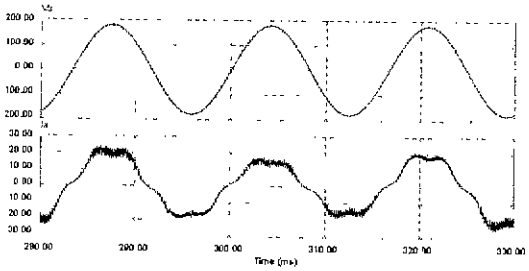

(b) input waveform filtered

Fig. 9 Input waveforms of proposed IAW(I)

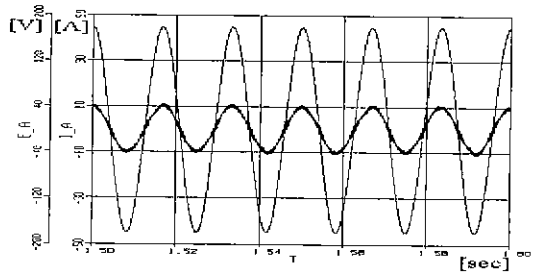

Fig. 10 Input waveforms of proposed IAW(II)

4.2 experiment

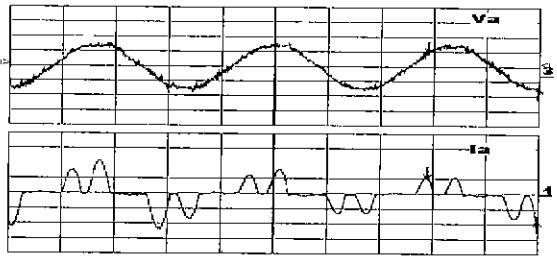

(a)input voltage(150V/div)/current(10A/div)

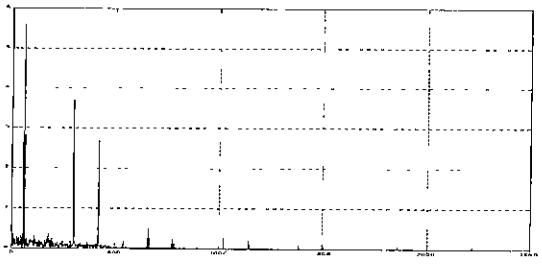

(b) FFT analysis of input current

Fig. 11 Input characteristics of conventional IAW

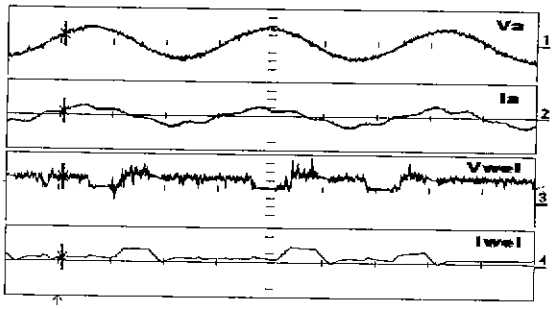

(a) input voltage/current

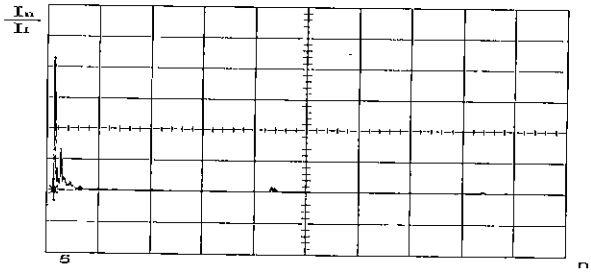

(b) FFT analysis of input current

Fig. 12 Input characteristics of proposed IAW(I)

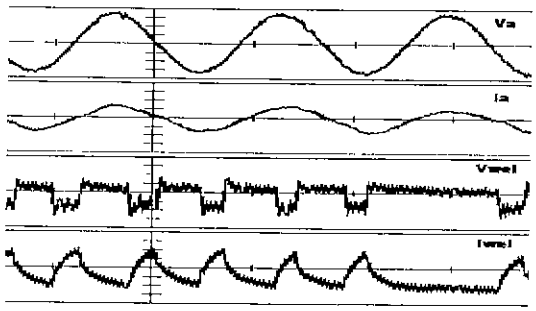

(a) input voltage/current

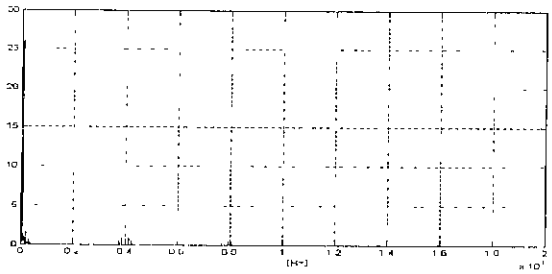

(b) FFT analysis of input current

Fig. 13 Input characteristics of proposed IAW(II)

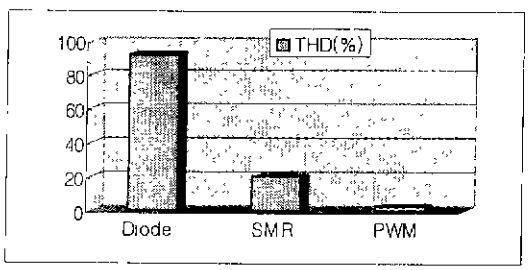

(a) THD

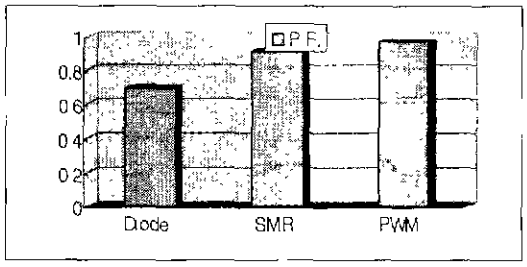

(b) power factor

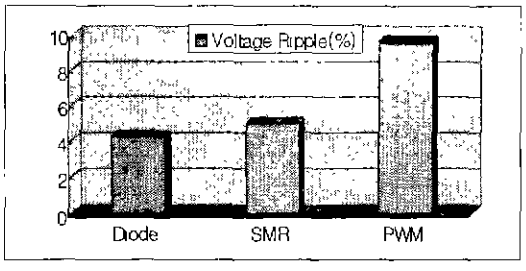

(c) votage ripple

Fig. 14 Comparison of input characteristics of IAW

Opcration and performance of the proposed IAWs are illustrated by the following experimental results. Fig.11 shows waveforms obtained from the conventional IAW. Comparing Fig.11, 12 and 13, it can be seen that low-order harmonics are eminently reduced in a IAW with the SMR or the PWM converter. The reduction of low-order harmonics results in power factor correction. Since the cost of IAW with the PWM converter is higher than that of IAW with SMR, it is reasonable to consider a trade off between cost and performance. The computational time of the current control is 125us when the DSP TMS320C31 is employed in PWM converter. Output voltage is selected as 400V considering the voltage rate of inverter and transformer. The Table 3. shows the comparisons of volume, weights and costs of IAWs. Also the performance comparison of IAWs is shown in Table 4.

Table 4. Comparison of experimental results

	conventional IAW	IAW with SMR	IAW with PWM
T.H.D[%]	91.75	20	2.63
P.F.	0.69	0.91	0.983
voltage ripple [%]	4.26	5.1	9.55
welding state	short metal transfer (arc voltage: 23V, arc current: 150A)		

5. Conclusion

IAWs with vltage source PWM converters have been described to evaluate the enhanced input characteristics in this paper. A comparison of input performance between IAWs has been performed on the base of THD, P.F, voltage ripple volume, volume and cost. The results of the experimental evaluation have shown that the proposed IAWs can significantly reduce THD and correct power factor. Voltage source PWM converters are suitable for IAW, and that are anticipated to enhance system performance even though additional control switches. However in a sence of dc ripple, a feedforward compensator must be designed to enhance dynamics characteristics. Research on the dynamics should be the object of future work.

Reference

[1] Y. M. Chae J. S. Gho G. H. Choe etc. "PWM Converter-Inverter Arc Welding Machine Using New Type N.C.T.", IEEE PESC, pp. 1636-1641, 1998.

[2] Mohammad Sadighy, Francis P. Dawson. "Single-Switched Three-Phase Power Factor Correction", IPEC- Yokohama, pp. 293-297, 1995.

[3] P. Kazmierkowski and Luigi Malesani, " Current Control Technique for Three-Phase Voltage-Source PWM Converter : A Survey", IEEE Trans. Indus. Elec., Vol. 45, No. 5, pp. 691-703, 1998.

[4] J. W. Kolar, H. Ertl and F. C. Zach, "Analysis of the control behavior of a bidirectional three-phase PWM rectifier system," EPE Conf.Rec. pp. 2-095-2-100, 1991.

[5] T. G. Habetler, "A Space Vector-Based Rectifier Regulator for AC/DC/AC Converters", IEEE Trans Power Elec., Vol. 8, No. 1, pp. 30-36, 1993.

[6] H S. Kim H. S. Mok G. H. Choe etc. "Design of Current Controller for 3-Phase PWM Converter with Unbalanced Input Voltage", IEEE PESC, pp. 503-509, 1998.